CHEMISTRY OF MATERIALS

Article

pubs.acs.org/cm

Bis-Aliphatic Hydrazone-Linked Hydrogels Form Most Rapidly at Physiological pH: Identifying the Origin of Hydrogel Properties with Small Molecule Kinetic Studies

Daniel D. McKinnon,[†,⊥,‡] Dylan W. Domaille,[†,‡] Jennifer N. Cha,*[,†] and Kristi S. Anseth*[,†,⊥,§]

[†]Department of Chemical and Biological Engineering, [⊥]BioFrontiers Institute, and [§]Howard Hughes Medical Institute, University of Colorado, Boulder, Colorado 80303, United States

Supporting Information

ABSTRACT: Rheological and small molecule kinetic studies were performed to study the formation and hydrolysis of the bis-aliphatic hydrazone bond. The rate of gelation was found to correspond closely with the rate of bond formation and the rate of gel relaxation with the rate of hydrolysis, indicating that small molecule kinetic studies can play an important role in material design. Furthermore, unlike aryl or acyl hydrazone bonds, the bis-aliphatic hydrazone bond forms rapidly under physiological conditions without requiring aniline catalysis yet maintains a pH-dependent rate of hydrolysis. These results suggest the bis-aliphatic hydrazone bond should find use alongside existing bioorthogonal click chemistries for bioconjugation, biomaterial synthesis, and controlled release applications.

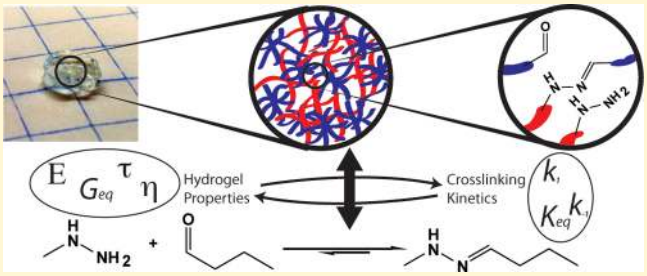

INTRODUCTION

Materials that behave predictably in response to applied stimuli have been employed in a myriad of advanced applications. For instance, functional materials that release payloads;[1−8] change geometries;[9,10] and alter their optical and mechanical properties in response to light,[11−15] heat,[16−18] pH,[10,17,19] electromagnetic fields,[20] and other stimuli[21] have been engineered for diverse applications ranging from differentiating stem cells[22,23] to simulating fracture healing[16] to directing cell migration.[24] Though various design strategies have been employed, organic polymer networks represent an especially utile class of stimuli-responsive materials because their properties can be easily and predictably modeled through established kinetic and polymer physics equations.[25−28] Furthermore, the defined functionalities of step growth polymer networks provide systems in which theoretical and experimental relationships can be more readily established between macroscopic material properties and cross-linking reaction kinetics.[29−31]

In previous work, we developed a cytocompatible covalently adaptable network formed through dynamically covalent hydrazone linkages, and we used the resulting material to explore the effects of a defined, viscoelastic microenvironment on cell behavior.[32] In the course of these studies, we observed the surprisingly fast gelation of a bis-aliphatic hydrazone cross-linked hydrogel and confirmed these results through a model kinetic study between an aliphatic hydrazine, monomethylhydrazine, and an aliphatic aldehyde, butyraldehyde. While hydrazone reactions have found widespread application in the fields of bioconjugation and materials science owing to their stimuli-responsive nature and their rapid formation under physiological conditions, when catalyzed by aniline or one of its derivatives,[33−37] most studies have focused on the reaction of aryl aldehydes with either aryl or acyl hydrazine partners.[33,34,36−39] Synthetically, these functionalities are easier to install in biological systems and, in the case of bis-aryl hydrazones, result in covalent linkages that are resistant to hydrolysis with corresponding equilibrium constants on the order of 10^6 M^{-1}.[38] However, as we and others have reported, the rate of formation and hydrolysis of aryl aldehyde derived hydrazones differ significantly from those of aliphatic aldehyde derived hydrazones, with the aliphatic hydrazone forming at a rate nearly 500-fold faster than a representative aryl hydrazone at neutral pH.[32,37,40] We reasoned that the kinetics of this reaction were heavily influencing the bis-aliphatic hydrazone hydrogel properties and sought to investigate how altering the kinetic and thermodynamic parameters of this chemical bond through changes in pH and temperature would influence the mechanical properties of a bis-aliphatic hydrazone cross-linked hydrogel (Figure 1).

Here, we present the effects of pH and temperature on the rheological properties of a bis-aliphatic hydrazone cross-linked hydrogel. We observed unexpectedly rapid hydrogel evolution at physiological pH and temperature and, in an effort to understand the origin of these characteristics, further explored this system by analyzing complementary small molecule kinetic studies. By reducing the complexity of the system to the reaction of model aliphatic aldehyde and hydrazine components, we were able to gain molecular insights into the origin of

Received: March 4, 2014
Revised: March 19, 2014

   dx.doi.org/10.1021/cm5007789 | Chem. Mater. XXXX, XXX, XXX−XXX

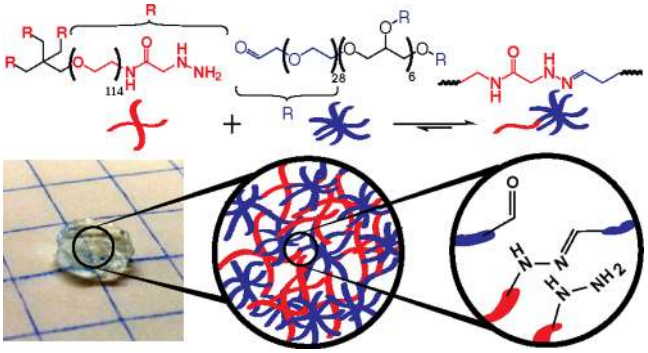

Figure 1. Gel formation occurs within minutes when 4-H and 8-AA are mixed due to the formation of the bis-aliphatic hydrazone bond cross-linking the polymer network.

the bulk hydrogel material properties. The forward and back rate constants of the small-molecule bis-aliphatic hydrazone reaction not only accurately describe the hydrogel evolution and stress relaxation properties but also suggest that the bis-aliphatic hydrazone bond should prove useful in a variety of research areas in which rapid and specific chemical ligation is desired, as the reaction exhibits a second-order rate constant that is competitive with specialized bioconjugation reactions.

EXPERIMENTAL SECTION

Macromer Synthesis. The 8-arm 10 kDa PEG-aldehyde (8-AA) was synthesized using a Swern oxidation.[41] Oxalyl chloride (88 equiv.) was dissolved in anhydrous DCM in a flame-dried flask purged with argon and immersed in a dry ice/acetone bath at −78 °C bath. Anhydrous DMSO (92 equiv.) was added dropwise, forming an activated alkoxy sulfonium intermediate. Next, one equivalent of 8-arm 10 kDa PEG-alcohol in a minimal volume of DCM was added dropwise, and the reaction was allowed to proceed for 20 min, at which point triethylamine (200 equiv.) was added dropwise. Finally, the reaction was allowed to warm to room temperature, and the product was precipitated with diethyl ether and purified by dialyzing against DI water. The 4-arm 20 kDa PEG-hydrazine (4-H) was synthesized by activating of triboc-hydrazinoacetic acid (8.8 equiv.) with HATU (8 equiv.) and *N*-methyl morpholine (18 equiv.) in DMF. One equivalent of 4-arm 20 kDa PEG-amine dissolved in DMF was added to the activated hydrazinoacetic acid solution, and the reaction was allowed to proceed overnight. Next, the product was precipitated in ether and dissolved in a 50:50 mixture of DCM/TFA to remove the Boc protecting group. After 4 h, the product was again precipitated in ether, dissolved in water, and dialyzed against DI water for 24 h. Finally, the product was lyophilized and used for experimentation.

Macromer Characterization. Macromers were characterized through ^{1}H NMR and shear rheology.

4-H ^{1}H NMR (D_2O, 400 MHz): δ = 3.59 (s, PEG).

4-H ^{1}H NMR (DMSO-d_6, 400 MHz): δ = 8.1 (t, J = 4 Hz, 1H), δ = 4.45 (m, 2H), δ = 3.51 (s, PEG), δ = 3.2 (m, 1H), δ = 2.96 (m, 2H).

8-AA ^{1}H NMR (D_2O, 400 MHz): δ = 5.04 (t, J = 6 Hz, 1H), δ = 3.76 (t, J = 4 Hz, 2H), δ = 3.59 (s, PEG). *Aldehyde exists as a diol in D_2O.*

8-AA ^{1}H NMR (DMSO-d_6, 400 MHz): δ = 9.61 (s, 1H), δ = 4.23 (s, 2H), δ = 3.54 (s, PEG). *8-AA gels in organic solvents; therefore, NMR peaks were significantly broadened.*

To determine functionalization, a four-arm benzaldehyde-terminated macromer of known functionalization was mixed with 4-H highly off-stoichiometrically, and the point at which gelation no longer occurred was noted. This information was combined with Flory–Stockmayer theory, which states[42]

$$p_c = \frac{1}{\sqrt{\frac{(f_A-1)(f_B-1)}{r}}}, \quad r = \frac{f_B n_B}{f_A n_A} \tag{1}$$

where f_A is the functionality of the first macromer, f_B is the functionality of the second macromer, n_B and n_A are their concentrations, and p_c is the percolation threshold, which must be greater than one for gelation to occur. For this system studied, f_A is 4 and f_B is 4, so theoretically, gelation should barely occur when the macromers are mixed 1:3.3 off-stoichiometrically. The result was observed, indicating that 4-H was nearly fully functionalized, which is not surprising given HATU-mediated peptide couplings are known to proceed to 99% completion.[43] The experiment was repeated with 4-H and 8-AA and similar results were observed, which is again expected as Swern oxidations are known to proceed to 97−100% to completion.[41]

Gel Formation. The PEG macromers were dissolved in buffered saline to form 30 wt % and 15 wt % stock solutions for the 4-arm PEG-hydrazine and 8-arm PEG-aldehyde, respectively. Solutions were combined stoichiometrically at 10.5 wt % to form hydrogels in situ on a temperature-controlled Peltier plate set to 25 °C on a shear rheometer, unless otherwise specified.

Rheology. Samples were formed in situ by pipetting 30 μL monomer solutions between the bottom Peltier plate and a flat tool 8 mm in diameter on a shear rheometer. The gap was closed to 500 μm as quickly as possible, and the experiment was commenced. All experiments were performed at 25 °C. Frequency and strain sweeps were performed to ensure measurements were made in the linear region. Evolution experiments were performed at 1% strain and 1 rad/s; frequency sweeps were performed at 1% strain, and stress relaxation experiments were performed at 10% strain.

Kinetics. An Eppendorf tube was charged with buffer at the indicated pH (198 μL), and butyraldehyde (1 μL of a 20 mM stock in DMSO) and methylhydrazine (1 μL of a 20 mM stock in DMSO) were added. The contents were quickly transferred to a cuvette, the cuvette was covered with a layer of Parafilm, and the absorbance at 240 nM was monitored (ε = 1986 M^{-1} cm^{-1}).[32] The data were fit to eq 2, a standard kinetic model derived by Dirksen et al.[33]

$$x(t) = \frac{a_+(x_0 - a_-) - a_-(x_0 - a_+)e^{-k_1(a_+ - a_-)t}}{(x_0 - a_-) - (x_0 - a_+)e^{-k_1(a_+ - a_-)t}} \tag{2}$$

$$a_+ = \frac{-k_{-1} + \sqrt{{k_{-1}}^2 + 4k_1k_{-1}x_0}}{2k_1}, \quad a_+ = \frac{-k_{-1} - \sqrt{{k_{-1}}^2 + 4k_1k_{-1}x_0}}{2k_1}$$

Here, x is the concentration of one reactant as a function of time; x_0 is the initial concentration of the reactant; k_1 and k_{-1} are the forward and backward rate constants; and $a+$ and $a-$ are defined in terms of these variables. This model assumes a bimolecular reaction with equimolar starting concentrations of the reactants and no side reactions. Each kinetic trace was fitted to the model, and the k_1 and k_{-1} values were recorded. Three independent measurements were made at each pH value. The reported values are the mean value and standard deviation for these three calculations. Excellent run-to-run agreement was seen at all pH values.

Rheological Modeling. Gel evolution was fit to an exponential model, as shown in eq 3

$$G(t) = G_\infty - Ae^{-\tau t} \tag{3}$$

where $G(t)$ is the elastic modulus, G_∞ is the equilibrium elastic modulus, A and τ are fit parameters, and t is the time. The half-lives of hydrogel evolution were calculated to compare the effects of different pH values.

Because every bond in the material is reversible, we assumed the material behaved as an ideal Maxwellian viscoelastic fluid, represented by a spring in series with a dashpot, as shown in Figure 2.

The total stress on a Maxwell material must equal the stress on each of the individual components, and the total strain is divided between the two with some time dependence. These assumptions are combined into eq 4

dx.doi.org/10.1021/cm5007789 | *Chem. Mater.* XXXX, XXX, XXX−XXX

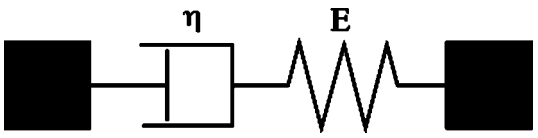

Figure 2. A dashpot (damper) with viscosity η in series with a spring of elastic modulus E is the simplest model for a viscoelastic fluid capable of capturing stress relaxation behavior.

$$\frac{d\varepsilon}{dt} = \frac{\sigma}{\eta} + \frac{1}{E}\frac{d\sigma}{dt} \quad (4)$$

where ε is the total strain, σ is the stress, η is the dashpot viscosity, E is the spring modulus, and t is the time. However, under the conditions used to measure stress relaxation, the material is strained a fixed amount and stress is measured; thus, the time derivative of strain is zero, and the equation simplifies to eq 5

$$\sigma(t) = \sigma_0 e^{-t/\tau} \quad (5)$$

where τ is a characteristic time constant of relaxation equal to the viscosity of the dashpot divided by the modulus of the spring. The stress relaxation data were then fit to this equation using the *FindFit* function in *Mathematica*, and relaxation times were used to quantitatively compare the effects of varying pH values.

Statistics. Small molecule kinetic studies were performed in triplicate, and rheological experiments were performed in duplicate. Error bars represent the standard deviation.

RESULTS AND DISCUSSION

Eight-arm 10 kDa and four-arm 20 kDa PEG macromers were functionalized with aliphatic aldehyde and hydrazine end-groups, respectively, using previously reported methods (Scheme 1).[32] Briefly, 8-arm PEG−OH was oxidized to its corresponding aliphatic aldehyde (8-AA) with a Swern oxidation procedure; precipitation from an ether solution provided the final material. Four-arm PEG-NH_2 was reacted with HATU-activated triboc-hydrazinoacetic acid to give the amide-linked aliphatic hydrazine (4-H). Treatment with DCM/TFA removed the Boc protecting groups, and subsequent precipitation from diethyl ether provided the final product.

Scheme 1. Synthetic Pathway to 8-arm 10 kDa Aliphatic Aldehyde (8-AA) and 4-arm 20 kDa Aliphatic Hydrazine (4-H)

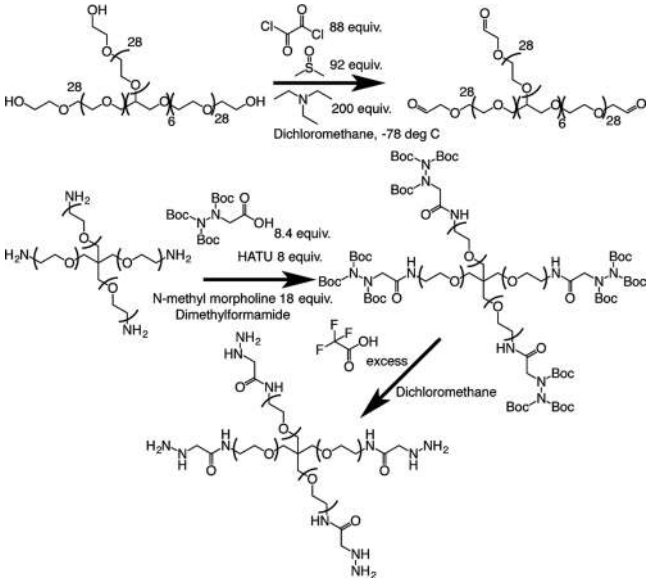

To investigate modulus evolution, bis-aliphatic hydrazone cross-linked hydrogels were formed in situ on the rheometer and shear viscous and elastic moduli were monitored as a function of time. Because hydrazone formation is canonically acid-catalyzed, we expected that the gels would form most rapidly at acidic pH and evolve more slowly as the pH increased. In contrast to our expectations, we observed relatively slow hydrogel formation at pH 4.2 and a maximal rate of gel evolution at physiological pH. Increasing the pH of the buffer above physiological pH led to a decrease in the rate of gel evolution (Figure 3A).

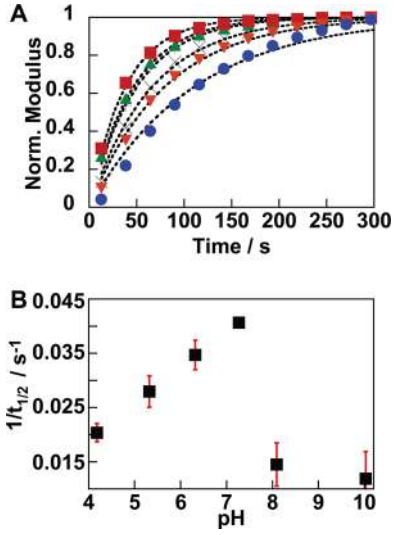

Figure 3. (A) Bis-aliphatic hydrazone hydrogel evolution traces at pH 4.2 (×), 5.3 (+), 6.3 (green ▲), 7.3 (red ■), 8.1 (orange ▼), and 10.0 (blue ●). Dashed lines represent a fit to an exponential model of step-growth hydrogel evolution. (B) Half-life of gel evolution at different pH values. Data points represent the average of two independent measurements. Error bars represent standard deviation.

Fitting the curves to eq 3, an exponential model of step-growth hydrogel evolution, yielded a half-life of gel evolution with respect to pH (Figure 3B). These half-lives are tabulated in Supporting Information Table 2 and show clearly that the hydrazone-linked hydrogel forms most rapidly at physiological pH; the rate of hydrogel formation drops off at more acidic and more basic pH values. While hydrogels formed at pH 4.2 require 50 s to reach half their equilibrium moduli, those at pH 7.3 require only 25 s, and those at pH 10.03 require 85 s (Figure 3B).

In an effort to better understand the unique rheological characteristics of the bis-aliphatic hydrazone hydrogels, we simplified the system to a model reaction between an aliphatic aldehyde, butyraldehyde, and an aliphatic hydrazine, monomethylhydrazine (Scheme 2).

We measured the rates of hydrazone formation between butyraldehyde and monomethylhydrazine in buffers identical to those used in the rheological characterization studies. Each kinetic trace was fitted independently to a second-order reversible kinetic model, derived by Dirksen et al.,[33] and this enabled the simultaneous determination of the forward (k_1) rate constant of hydrazone formation and the back rate

dx.doi.org/10.1021/cm5007789 | *Chem. Mater.* XXXX, XXX, XXX−XXX

Scheme 2. The Small Molecule Reaction between Monomethylhydrazine and Butyraldehyde Was Used as a Model System[a]

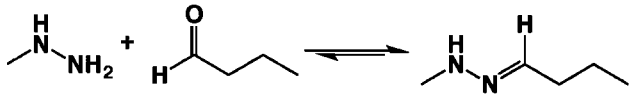

[a]Reaction progress was monitored by measuring the absorbance at 240 nm.

constant (k_{-1}) of hydrazone hydrolysis at each pH condition (Figure 4A).

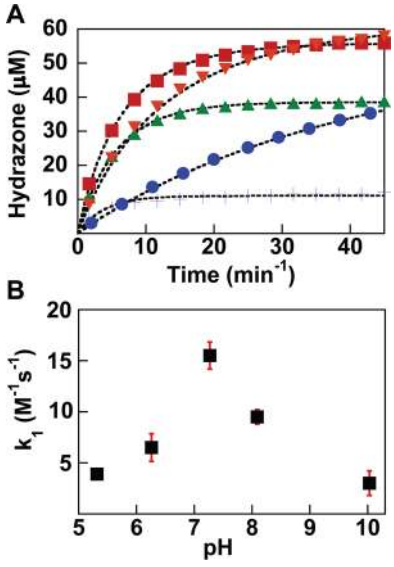

Figure 4. (A) Hydrazone formation between butyraldehyde (100 μM) and monomethylhydrazine (100 μM) at 5.3 (+), 6.3 (green ▲), 7.3 (red ■), 8.1 (orange ▼), and 10.0 (blue ●). Dashed lines represent a fit to a second-order reversible reaction model.[33] (B) Second-order rate constant for hydrazone formation between butyraldehyde and monomethylhydrazine at different pH values. Each data point represents the average of three independent kinetic measurements. Error bars represent standard deviation.

As the pH of the solution increased from 5.3 to 6.3, we saw an increase in the rate of small molecule hydrazone formation, from 3.9 ± 0.5 M^{-1} s^{-1} at pH 5.3 to 6.5 ± 1.4 M^{-1} s^{-1} at pH 6.3. In excellent agreement with the hydrogel evolution studies, we saw maximal hydrazone formation at pH 7.3, with a corresponding forward rate constant of 15.5 ± 1.3 M^{-1} s^{-1}. Again, in agreement with the hydrogel evolution studies, the rate of hydrazone formation decreased as the pH was increased above physiological pH. Increasing the pH to 8.1 led to a decrease in rate relative to the rate at pH 7.3, but hydrazone formation still proceeded remarkably fast, with a second-order rate constant of 9.5 ± 0.7 M^{-1} s^{-1}. Even in pH 10.0 phosphate buffer, we observed rapid hydrazone formation, with a corresponding forward rate constant of 3.0 ± 1.2 M^{-1} s^{-1} (Figure 4B). The correlation between the small molecule studies and the hydrogel evolution traces strongly suggests that the rate of hydrogel evolution is dominated by the kinetics of the of bis-aliphatic hydrazone formation.

Because the bis-aliphatic hydrazone bond is reversible and the kinetics of the hydrolysis reaction vary significantly with pH, we next sought to investigate the pH-dependent stress relaxation properties of the material. We previously postulated that the stress relaxation properties would be heavily influenced by the rate of hydrazone bond hydrolysis.[32] Thus, by studying the stress relaxation properties over a range of pH values, we sought to directly interrogate the effect of hydrazone hydrolysis on the mechanical properties of the gel. We again formed hydrogels in situ and allowed them to equilibrate for 30 min in a buffered bath before straining to 10% at 25 °C. Stress was recorded as a function of time, and a clear pH-dependent behavior was observed, with the rate of stress relaxation increasing as a function of proton concentration (Figure 5A).

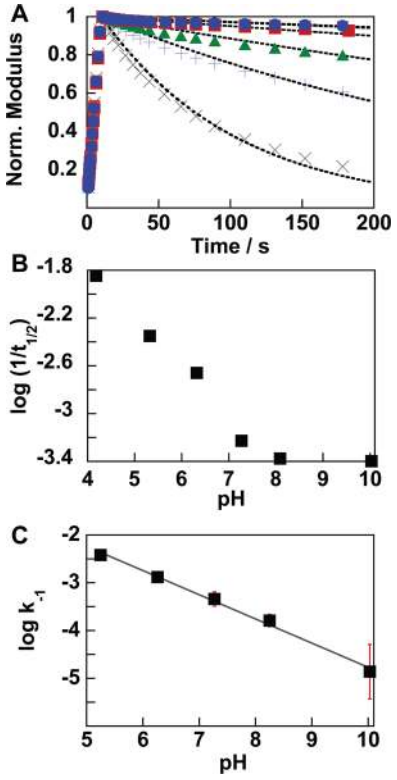

Figure 5. (A) Hydrogel stress relaxation at pH 4.2 (×), 5.3 (+), 6.3 (green ▲), 7.3 (red ■), 8.1 (orange ▼), and 10.0 (blue ●). Dashed lines represent a fit to the Maxwell model.[42] (B) Inverse half-life of gel relaxation at different pH values. (C) Rate of small molecule hydrazone hydrolysis at different pH values. Each data point represents the average of three independent kinetic measurements. Error bars represent standard deviation.

The relaxation traces were fit to the Maxwell model (Figure 2), which assumes the material behaves as an elastic spring placed in series with a viscous dashpot; this represents the simplest model capable of predicting stress relaxation.[42] This fitting provided the time constants of relaxation, τ, which spanned more than an order of magnitude, from 300 s at pH 4.2 to 4000 s at pH 10.0 (Figure 4B). The fits are shown in Figure 4A, and the excellent agreement between the model and the data indicate that changes in pH do not introduce network nonidealities and that the relaxation properties can be predictably controlled through pH modulation.

The kinetic treatment of the hydrazone evolution studies between butyraldehyde and monomethylhydrazine also provides the rate of the back reaction, k_{-1}, which corresponds to the hydrolysis of the hydrazone bond. Plotting the rate of the back reaction with respect to pH provided good agreement

dx.doi.org/10.1021/cm5007789 | *Chem. Mater.* XXXX, XXX, XXX−XXX

with the rheological data: more acidic buffers greatly enhances the rate of hydrolysis, an observation in line with previous studies of hydrazone hydrolytic stability (Figure 4C).[44] As the rate of k_{-1} decreases, a factor that can be precisely altered by increasing the pH, the gels take longer to relax applied stress; at more acidic pH values, the k_{-1} values increase, and correspondingly, the gels relax stress more quickly. Thus, the rate of the back reaction dominates the ability of the material to relax applied stress, an observation that should provide a valuable design principle for the development of next-generation stress relaxation materials.

Taken together, the small molecule kinetic studies provide excellent agreement with the hydrogel evolution and stress relaxation characteristics of bis-aliphatic hydrazone hydrogels. It is notable that the rheological characteristics of a complex PEG hydrogel system can be captured by the characteristics of the kinetics of the reactive end groups. This demonstration provides a versatile strategy for screening of suitable hydrogel-forming reactions through analogous small-molecule studies, and future studies will focus on quantifying the theoretical underpinnings of the relationship between the relaxation properties of the hydrogel and the rate constants of the cross-linking reactions.

CONCLUSIONS

To close, our study demonstrates that a small-molecule model system can capture and describe the origin of bis-aliphatic hydrazone hydrogel evolution and stress relaxation characteristics. The forward rate constant of the reaction dominates the gel evolution process, while the back rate constant heavily influences the ability of the gel to relax stress, providing a set of rational design principles for the development of next-generation stress relaxation materials. Moreover, the unexpectedly rapid formation of the bis-aliphatic hydrazone at physiological pH indicates that this reaction may find extensive use in bioconjugation methods and dynamic covalent chemistry applications, especially for use with pH-sensitive proteins and molecules.

ASSOCIATED CONTENT

Supporting Information

A discussion of the rapid formation of the bis-aliphatic hydrazone bond, recipes for buffers used, temperature dependence on hydrogel stress relaxation, and raw kinetic values. This material is available free of charge via the Internet at http://pubs.acs.org.

AUTHOR INFORMATION

Corresponding Authors

*E-mail: Jennifer.Cha@colorado.edu.
*E-mail: Kristi.Anseth@colorado.edu.

Author Contributions

‡D.D.M. and D.W.D. contributed equally.

Funding

Office of Naval Research (N00014−13−1−0283), the National Science Foundation (CBET 1236662), and the Howard Hughes Medical Institute funded this work.

Notes

The authors declare no competing financial interest.

ACKNOWLEDGMENTS

The authors acknowledge Drs. Kelly Schultz and Malar Azagarsamy for helpful discussions.

ABBREVIATIONS

PEG, poly(ethylene glycol); DMF, dimethylformamide; DCM, dichloromethane; 8-AA, 8-arm 10 kDa aliphatic aldehyde-terminated PEG macromer; 4-H, 4-arm 20 kDa aliphatic hydrazine-terminated PEG macromer; DMSO, dimethyl sulfoxide; HATU, (1-[bis(dimethylamino)methylene]-1*H*-1,2,3-triazolo[4,5-b]pyridinium 3-oxid hexafluorophosphate; TFA, trifluoroacetic acid

REFERENCES

(1) Gillies, E. R.; Fréchet, J. M. J. *Bioconjugate Chem.* **2005**, *16*, 361−368.
(2) Gillies, E. R.; Jonsson, T. B.; Fréchet, J. M. J. *J. Am. Chem. Soc.* **2004**, *126*, 11936−11943.
(3) Azagarsamy, M. A.; Alge, D. L.; Radhakrishnan, S. J.; Tibbitt, M. W.; Anseth, K. S. *Biomacromolecules* **2012**, *13*, 2219−2224.
(4) Azagarsamy, M. A.; Anseth, K. S. *Angew. Chem., Int. Ed.* **2013**, *52*, 13803−13807.
(5) Griffin, D. R.; Kasko, A. M. *J. Am. Chem. Soc.* **2012**, *134*, 13103−13107.
(6) Griffin, D. R.; Kasko, A. M. *ACS Macro Lett.* **2012**, *1*, 1330−1334.
(7) Chang, B.; Chen, D.; Wang, Y.; Chen, Y.; Jiao, Y.; Sha, X.; Yang, W. *Chem. Mater.* **2013**, *25*, 574−585.
(8) Jing, J.; Szarpak-Jankowska, A.; Guillot, R.; Pignot-Paintrand, I.; Picart, C.; Auzély-Velty, R. *Chem. Mater.* **2013**, *25*, 3867−3873.
(9) Kim, J.; Hanna, J. A.; Byun, M.; Santangelo, C. D.; Hayward, R. C. *Science* **2012**, *335*, 1201−1205.
(10) Rodríguez-Hernández, J.; Lecommandoux, S. *J. Am. Chem. Soc.* **2005**, *127*, 2026−2027.
(11) Kloxin, A. M.; Kasko, A. M.; Salinas, C. N.; Anseth, K. S. *Science* **2009**, *324*, 59−63.
(12) Scott, T. F.; Schneider, A. D.; Cook, W. D.; Bowman, C. N. *Science* **2005**, *308*, 1615−1617.
(13) Guvendiren, M.; Burdick, J. A. *Nat. Commun.* **2012**, *3*, 792.
(14) Khetan, S.; Guvendiren, M.; Legant, W. R.; Cohen, D. M.; Chen, C. S.; Burdick, J. A. *Nat. Mater.* **2013**, *12*, 458−465.
(15) Gumbley, P.; Koylu, D.; Pawle, R. H.; Umezuruike, B.; Spedden, E.; Staii, C.; Thomas, S. W., III *Chem. Mater.* **2014**, *26*, 1450−1456.
(16) Chen, X.; Dam, M. A.; Ono, K.; Mal, A.; Shen, H.; Nutt, S. R.; Sheran, K.; Wudl, F. *Science* **2002**, *295*, 1698−1702.
(17) Zhang, J.; Peppas, N. A. *Macromolecules* **2000**, *33*, 102−107.
(18) Dong, H.; Mantha, V.; Matyjaszewski, K. *Chem. Mater.* **2009**, *21*, 3965−3972.
(19) Deng, G.; Tang, C.; Li, F.; Jiang, H.; Chen, Y. *Macromolecules* **2010**, *43*, 1191−1194.
(20) Adzima, B. J.; Kloxin, C. J.; Bowman, C. N. *Adv. Mater.* **2010**, *22*, 2784−2787.
(21) Sidorenko, A.; Krupenkin, T.; Taylor, A.; Fratzl, P.; Aizenberg, J. *Science* **2007**, *315*, 487−490.
(22) Wang, H.; Haeger, S. M.; Kloxin, A. M.; Leinwand, L. A.; Anseth, K. S. *PLoS One* **2012**, *7*, e39969.
(23) Wang, H.; Tibbitt, M. W.; Langer, S. J.; Leinwand, L. A.; Anseth, K. S. *Proc. Nat. Acad. Sci.* **2013**, *110*, 19336−19341.
(24) Wylie, R. G.; Ahsan, S.; Aizawa, Y.; Maxwell, K. L.; Morshead, C. M.; Shoichet, M. S. *Nat. Mater.* **2011**, 799−806.
(25) Flory, P. J. *J. Am. Chem. Soc.* **1941**, *63*, 3083−3090.
(26) Flory, P. J. *J. Phys. Chem.* **1942**, *46*, 132−140.
(27) Flory, P. *Polymer* **1979**, *20*, 1317−1320.
(28) Baxandall, L. G. *Macromolecules* **1989**, *22*, 1982−1988.
(29) Metters, A. T.; Bowman, C. N.; Anseth, K. S. *J. Phys. Chem. B* **2000**, *104*, 7043−7049.
(30) Metters, A. T.; Anseth, K. S.; Bowman, C. N. *J. Phys. Chem. B* **2001**, *105*, 8069−8076.

(31) Metters, A.; Hubbell, J. *Biomacromolecules* **2005**, *6*, 290−301.
(32) McKinnon, D. D.; Domaille, D. W.; Cha, J. N.; Anseth, K. S. *Adv. Mater.* **2014**, *26*, 865−872.
(33) Dirksen, A.; Dirksen, S.; Hackeng, T. M.; Dawson, P. E. *J. Am. Chem. Soc.* **2006**, *128*, 15602−15603.
(34) Dirksen, A.; Dawson, P. E. *Bioconjugate Chem.* **2008**, *19*, 2543−2548.
(35) Domaille, D. W.; Lee, J. H.; Cha, J. N. *Chem. Commun.* **2013**, *49*, 1759−1761.
(36) Crisalli, P.; Kool, E. T. *J. Org. Chem.* **2013**, *78*, 1184−1189.
(37) Kool, E. T.; Park, D.-H.; Crisalli, P. *J. Am. Chem. Soc.* **2013**, *135*, 17663−17666.
(38) Dirksen, A.; Yegneswaran, S.; Dawson, P. E. *Angew. Chem., Int. Ed.* **2010**, *49*, 2023−2027.
(39) Blanden, A. R.; Mukherjee, K.; Dilek, O.; Loew, M.; Bane, S. L. *Bioconjugate Chem.* **2011**, *22*, 1954−1961.
(40) Nguyen, R.; Huc, I. *Chem. Commun.* **2003**, 942−943.
(41) Omura, K.; Swern, D. *Tetrahedron Lett.* **1978**, *34*, 1651−1660.
(42) Rubinstein, M.; Colby, R. H. *Polymer Physics*; Oxford University Press: New York, 2003.
(43) Carpino, L. A.; El-Faham, A.; Minor, C. A.; Albericio, F. *J. Chem. Soc., Chem. Commun.* **1994**, *0*, 201−203.
(44) Kalia, J.; Raines, R. T. *Angew. Chem., Int. Ed.* **2008**, *47*, 7523−7526.